Hα Dimming Associated With the Eruption of a Coronal Sigmoid in the Quiet Sun

Yunchun Jiang · Huadong Chen · Yuandeng Shen · Liheng Yang · Kejun Li

Abstract We report on the occurrence of Hα dimming associated with a sigmoid eruption in a quiet-sun region on 14 August 2001. The coronal sigmoid in soft X-ray images from the *Yohkoh* Soft X-ray Telescope was located over an Hα filament channel. Its eruption was accompanied by a flare of GOES X-ray class C2.3 and possibly associated with a halo coronal mass ejection (CME) observed with the *Large Angle and Spectroscopic Coronagraphs* (LASCO) on board the *Solar and Heliospheric Observatory* (SOHO). During the eruption, coronal bipolar double dimming took place at the regions with opposite magnetic polarities around the two sigmoid ends, but the underlying chromospheric channel did not show observable changes corresponding to the coronal eruption. Different from the erupting coronal sigmoid itself, however, the coronal dimming had a detectable chromosphere counterpart, *i.e.*, Hα dimming. By regarding the sigmoid as a coronal sign for a flux rope, these observations are explained in the framework of the flux rope model of CMEs. The flux rope is possibly deeply rooted in the chromosphere, and the coronal and Hα dimming regions mark its evacuated feet, through which the material is possibly fed to the halo CME.

1. Introduction

Coronal mass ejections (CMEs), sudden eruptions of magnetized plasma from the solar corona into the interplanetary space, represent a large-scale rearrangement of coronal magnetic fields. Since "halo" CMEs, showing up as diffuse ring-like structures beyond the edge of the occulting disk, can be related to Earth-directed CMEs and can lead to major interplanetary transient with significant geomagnetic effects, they seem to be the most important CMEs from a space weather standpoint. Observations of the early on-disk CME signatures are important in detecting Earth-directed CMEs and in understanding the initiation and generation mechanism of CMEs, but the connection between Earth-directed CMEs and their on-disk source regions remains to be established.

Y. Jiang (✉) · H. Chen · Y. Shen · L. Yang · K. Li
National Astronomical Observatory/Yunnan Astronomical Observatory, Chinese Academy of Sciences, P.O. Box 110, Kunming 650011, China
e-mail: jyc@ynao.ac.cn

As a key coronal signature of CMEs, coronal dimming events have recently received considerable attention (Hudson, Acton, and Freeland, 1996; Gopalswamy and Hanaoka, 1998; Thompson *et al.*, 1998; Harrison and Lyons, 2000; Harra and Sterling, 2001; Jiang *et al.*, 2006). They are often associated with other common forms of the on-disk CME signatures, such as flares, filament eruptions, eruptions of coronal sigmoid structures, and so on (Hudson and Cliver, 2001). In some halo events (see Sterling and Hudson, 1997; Zarro *et al.*, 1999, and the references therein), coronal dimming regions have been identified as the on-disk CME source regions by using observations from the *Yohkoh* Soft X-ray Telescope (SXT) and the *Solar and Heliospheric Observatory* Extreme Ultraviolet Telescope (SOHO/EIT) and are interpreted to represent a drop in density instead of a decrease in temperature since they have typical time scales from an hour to several days, which is shorter than the typical radiative time scale in the corona. These coronal dimming regions show varying forms (Hudson and Webb, 1997), and in particular they sometimes take the form of the so-called bipolar double dimming with two coronal dimming regions located above the opposite magnetic polarities (see Thompson *et al.*, 2000; Jiang, Li, and Yang, 2006, and the references therein). It is believed that bipolar double dimming represents the footprints of a large-scale flux rope ejection and the plasma mass that is lost from the corona and swept into the CME.

In some CME events, similar coronal dimming features were detected in SXT and EIT images, which represent different temperature regimes. In two halo events studied by Wang *et al.* (2000), however, the coronal dimming clearly appeared in EIT 195 Å but was not seen in SXT soft X rays. More recently, Jiang *et al.* (2003) first reported that the coronal dimming can extend deeply into the chromosphere and forms obvious Hα dimming, the optical counterpart of coronal dimming. The Hα dimming is different from the flare nimbus phenomenon, an Hα dark halo seen around major flares discovered by Ellison, Mckenna, and Reid (1961), and also from the Hα darkening lying outside but adjacent to the bright flare emission in major flares first noticed by Neidig *et al.* (1997). In the event studied by Jiang *et al.* (2003), the coronal and corresponding Hα dimming regions had a similar shape and took the form of bipolar double dimming. They were associated with a violent eruption of an active region filament, an intensive X-ray class X1.6 flare, and a halo CME. By now, only this one example of Hα dimming events was found, so that further study is needed to understand their origin. For example, a natural question is whether Hα dimming also takes place during more gentle eruption occurring in quiet-sun regions. In this paper, we make a comparative study, focusing on another example of Hα dimming events that took place during the eruption of a sigmoidal structure overlying a large quiescent filament channel in the quiet sun. This eruption, occurring on 14 August 2001, was associated with an X-ray class C2.3 flare, a coronal bipolar double dimming, and a halo CME observed by the *Large Angle and Spectroscopic Coronagraphs* (LASCO) on SOHO (SOHO/LASCO). By combining Hα, EUV, soft X-ray, and corresponding magnetic field data, we will show that the coronal dimming also had corresponding Hα dimming.

2. Observations

For the present study, we used the following data:

1. Full-disk Hα line center images from the global Hα five-station network (Steinegger *et al.*, 2000). The stations are Big Bear Solar Observatory (BBSO) in the USA, Kanzelhöhe Solar Observatory (KSO) in Austria, Catania Astrophysical Observatory in Italy, and the Yunnan Astronomical Observatory and Huairou Solar Observing Station in China. The
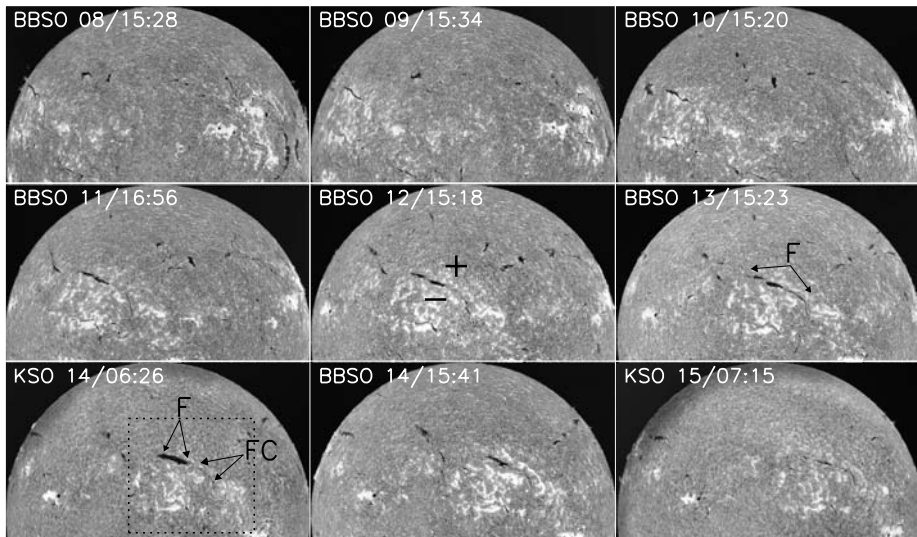
Figure 1 Hα center-line images from August 8 to 15, showing the daily appearance of the quiescent filament underlying the coronal sigmoid. The area inside the black box marks the field of view (FOV) of Figure 2.

observations at KSO and BBSO covered the event well. The KSO's (BBSO's) images are acquired using a Zeiss (Halle) Lyot filter with a bandpass of ± 0.7 Å (± 0.5 Å) and are recorded by a 2048×2048 Apogee 14 bit KX4 camera. The cadence of the Hα images is 1 minute, and the pixel size is roughly $1''$, which yields a spatial resolution of $2''$. Daily Hα data from other stations are also examined.

2. *Yohkoh*/SXT full-disk soft X-ray images in the wavelength range of $3-50$ Å ($2-4 \times 10^6$ K) (Tsuneta *et al.*, 1991). The SXT data used for the sigmoid eruption were taken through the Al/Mg/Mn and Al.l filters at the half-resolution mode ($4.9''$ per pixel) in a various cadence.

3. SOHO/EIT full-disk 304 Å (He II, 6×10^4 K), 171 Å (Fe IX/X, 1×10^6 K), 195 Å (Fe XII, 1.5×10^6 K), and 284 Å (Fe XV, 2×10^6 K) images with a spatial resolution of $2.6''$ per pixel (Delaboudiniére *et al.*, 1995) and the C3 white-light coronagraph data from SOHO/LASCO, which covers the range of 4 to 32 solar radii (Brueckner *et al.*, 1995). On 2000 August 14, all EIT 195 Å and LASCO data between 01:30 and 15:30 UT were lost owing to an instrument problem, but the EIT EUV images from the synoptic sets (taken four times daily) are available.

4. Line-of-sight magnetograms from the Michelson Doppler Imager (MDI) on SOHO (Scherrer *et al.*, 1995). For the current study, MDI provides full-disk longitudinal magnetograms with a pixel size of $2''$ and a cadence of 96 minutes.

3. Results

An eruptive coronal sigmoid structure was located on the quiet-sun region in the northern hemisphere. On August 14, its centroid was at around N26W10 and overlaid an Hα filament channel. Figure 1 shows the daily appearance of the quiescent filament channel from August 8 to 15, in which the positive and negative signs indicate the corresponding magnetic

polarities in the photosphere divided by the filament channel. Figure 2 shows the general evolution of the sigmoid eruption in KSO and BBSO Hα, SXT soft X-ray, and EIT 195 Å observations. As expected, the filament channel laid along a polarity inversion line of photospheric magnetic fields. It stayed visible during its passage across the solar disk although there were some morphological changes and part of a filament came and went in the whole filament channel. On August 13, the whole filament channel was occupied by a single dark filament (labeled as F in Figure 1). On August 14 before the sigmoid eruption, however, the filament was divided into two parts connected with each other (see Figure 1). Its northeastern part became darker and thicker (labeled as F in Figure 2), while its southwestern part was substituted by a section of the filament channel (labeled as FC in Figure 2), along which Hα fibrils were arranged in order but no clear dark filament was seen. In soft X-ray images, the eruptive sigmoid structure was located just above the filament channel (indicated by the white arrows in the frame at 07:30 UT in Figure 2b) while some left-skewed soft X-ray loops were seen above the filament section F (indicated by the black arrow in the frame at 09:19 UT in Figure 2b). The sigmoid and the left-skewed loops can be clearly distinguished from each other. Like the case studied by Pevtsov, Canfield, and Zirin (1996), we note that both the filament channel and the coronal sigmoid exhibited a similar inverse-S shape, suggesting that they might belong to the same topological structure. This is consistent with the finding of Pevtsov (2002) that there is a close spatial association between chromospheric filament channels and coronal sigmoids. According to the definition of Martin, Bilimoria, and Tracadas (1994), we can identify the filament channel as a dextral one. Therefore, identifications of the left-skewed loops, the dextral filament channel, and the inverse-S sigmoid were also consistent with the preferential hemispheric pattern of chirality (Zirker *et al.*, 1997; Martin, 1998).

The sigmoid eruption was accompanied by a flare of GOES X-ray class C2.3 with start, peak, and end times of 11:30, 12:42, and 14:04 UT, respectively (see the GOES-8 $1-8$ Å soft X-ray flux profile in Figure 5a). In SXT observations, the sigmoid and the left-skewed loops were obviously disturbed before the GOES flare onset (see the frame at 10:58 UT in Figure 2b). Then the sigmoid completely disappeared, and a postflare arcade (labeled as PFA in Figure 2) was formed to gradually straddle the whole Hα filament channel. Therefore, the preflare left-skewed loops were also replaced by the arcade. In Hα observations, the Hα flare consisted of two distinct ribbons located in regions of opposite polarity on both sides of the filament channel, which can be clearly discernible at the GOES flare start (see the arrows in the frame at 11:30 UT in Figure 2a). Similar to the situation of classical two-ribbon flares associated with filament eruptions, the two ribbons were nearly parallel to the polarity inversion line, showing a clear increase in separation with time. As in the six cases studied by Pevtsov (2002), however, a striking characteristic of the eruption is that the whole filament channel had no obvious changes throughout the flare duration in which the major coronal disturbances happened. By the GOES flare maximum (12:42 UT), neither the filament nor the filament channel looked clearly different from those at the GOES flare start time (11:30). After the GOES flare end (14:04 UT), the filament gradually disappeared, but it is clear that this disappearance was possibly the result and not the cause of the flare. In EIT 195 Å observations, the flare ribbons and postflare arcade were also seen and showed similar appearance and consistent evolution (Figure 2c).

Another remarkable characteristic of the sigmoid eruption is that two obvious coronal dimming regions, "CDR1" and "CDR2", were formed during the eruption. In soft X-ray images, the commencements of the dimming were nearly simultaneous with the activation of the sigmoid at 10:58 UT before the GOES flare start (indicated by the white arrows in
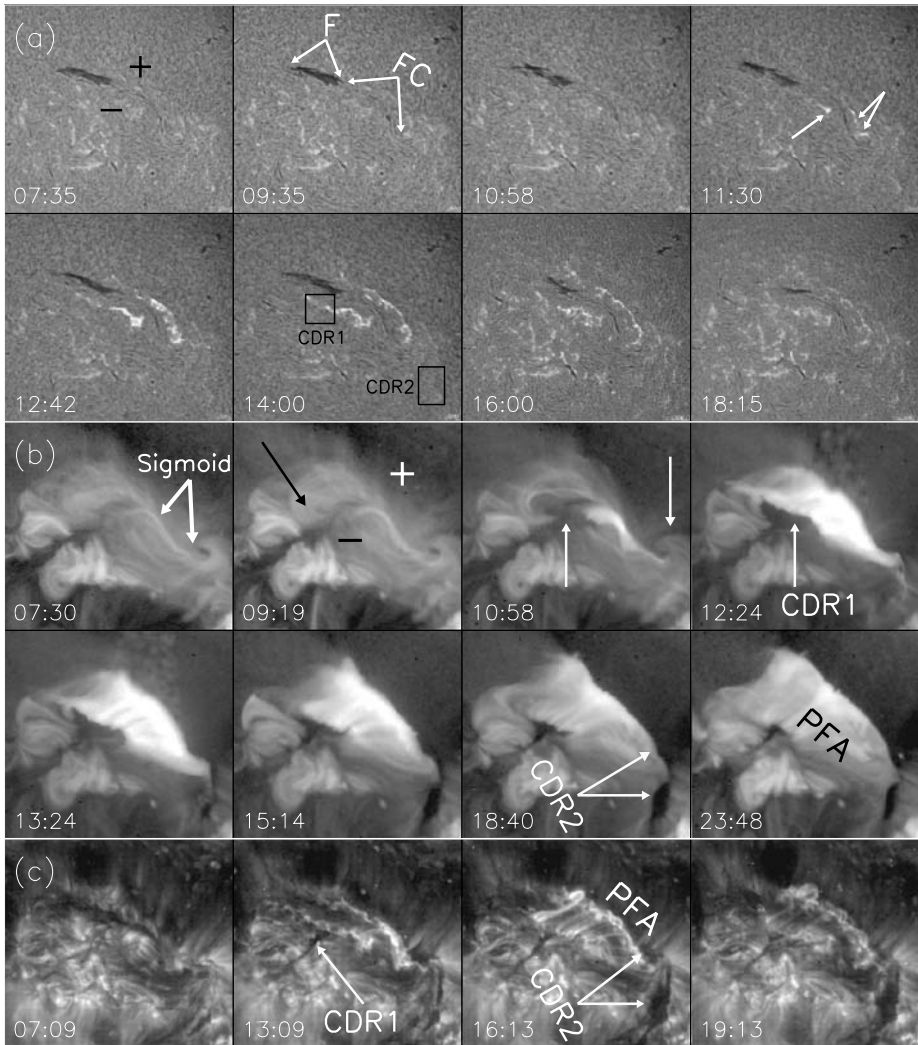
Figure 2 Hα center-line (a), *Yokoh*/SXT soft X-ray (b) and EIT 195Å (c) images of the sigmoid eruption. "+" and "−" signs mark the corresponding (positive and negative) magnetic polarities in the photosphere. The FOV, indicated by the box in Figure 1, is $790'' \times 720''$.

the frame at 10:58 UT in Figure 2b). Subsequently, CDR1 and CDR2 showed different evolution. CDR1 reached its maximum size at 12:24 UT after a *Yokoh* night, then gradually decreased in area since the footpoints of the postflare arcade expanded away from the polarity inversion line and completely disappeared after about 04:00 UT of the next day. CDR2, however, gradually developed toward the south after 12:24 UT, reached its maximum size at about 18:40 UT, then slowly shrank and eventually disappeared at 07:00 UT of the next day. Although no continuous EIT observations were available, both CDR1 and CDR2 were definitely seen in 195 Å images. Figure 3 shows difference images with pre-event images subtracted from those after the sigmoid eruption at 304 Å (Figure 3b), 195 Å (Figure 3c),

Figure 3 MDI line-of-sight magnetogram (a), EIT 304 Å (b), EIT 195 Å (c), EIT 284 Å (d), SXT soft X-ray (e), and Hα (f) difference images. The two coronal dimming regions, CDR1 and CDR2, are located on the regions of opposite magnetic polarities and are superposed as black and white contours in panel (a). The boxes in panel f mark the areas in which the Hα light curves are measured and displayed in Figure 5. The FOV is the same as in Figure 2.
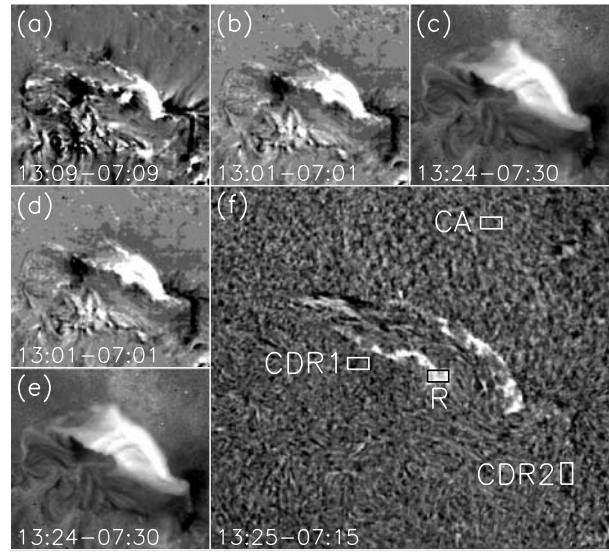
284 Å (Figure 3d), soft X rays (Figure 3e), and Hα (Figure 3f). Both CDR1 and CDR2 were clearly seen and showed similar shapes in soft X-ray, 195 Å, and 284 Å difference images. They were located around the two ends of the eruptive sigmoid and above the regions of opposite magnetic polarities, with CDR1 over a negative region and CDR2 over a positive region. Thus, as in the cases studied by a number of authors in some halo events (Sterling and Hudson, 1997; Zarro *et al.*, 1999; Jiang *et al.*, 2003; Jiang, Li, and Yang, 2006), both CDR1 and CDR2 were composed of bipolar double dimming. Moreover, CDR1 and CDR2 were also quite obvious in 304 Å and Hα difference images. Therefore, as in the case of chromospheric dimming in a halo event (Jiang *et al.*, 2003), the coronal dimming in CDR1 and CDR2 might deeply extend into the chromosphere. This was confirmed by examining high-cadence Hα observations from KSO and BBSO. Figure 4 presents the close-up view of Hα images below and around CDR1 and CDR2. There were two chromospheric Hα plages (indicated by the black arrows) below CDR1 and CDR2 before the sigmoid eruption. We see that their brightness became fainter and fainter, and their nearby areas (indicated by the thick white arrows) became darker and darker in the course of the eruption. Therefore, we believe that the Hα dimming, the chromospheric counterpart of the coronal dimming, indeed occurred. It is noted that the two chromospheric plage regions were located over regions of opposite magnetic polarity in the photosphere with field strengths stronger than nearby background. Unfortunately, the low cadence of the MDI magnetogram observations in this event does not allow us to examine the possible change of photospheric magnetic fields associated with the Hα dimming. The light curves of Hα intensities in three boxes centered on the two dimming regions (white boxes, "CDR1", and "CDR2", in Figure 3f and Figure 4) and one of the flare ribbons (black box, "R", in Figure 3f) are measured and plotted in Figure 5. To account for intensity changes from atmospheric seeing, the three boxes are chosen to be equal in size and the intensity measurements are calibrated to the mean intensity of a control area with the same size but outside the dimming and flare regions (white box, "CA", in Figure 3f). We see that the Hα flare brightening and the Hα dimming simultaneously started at about 11:00 UT, which was slightly prior to the GOES flare onset time at 11:30 UT. This was consistent with the sigmoid activation and the appearance of coronal
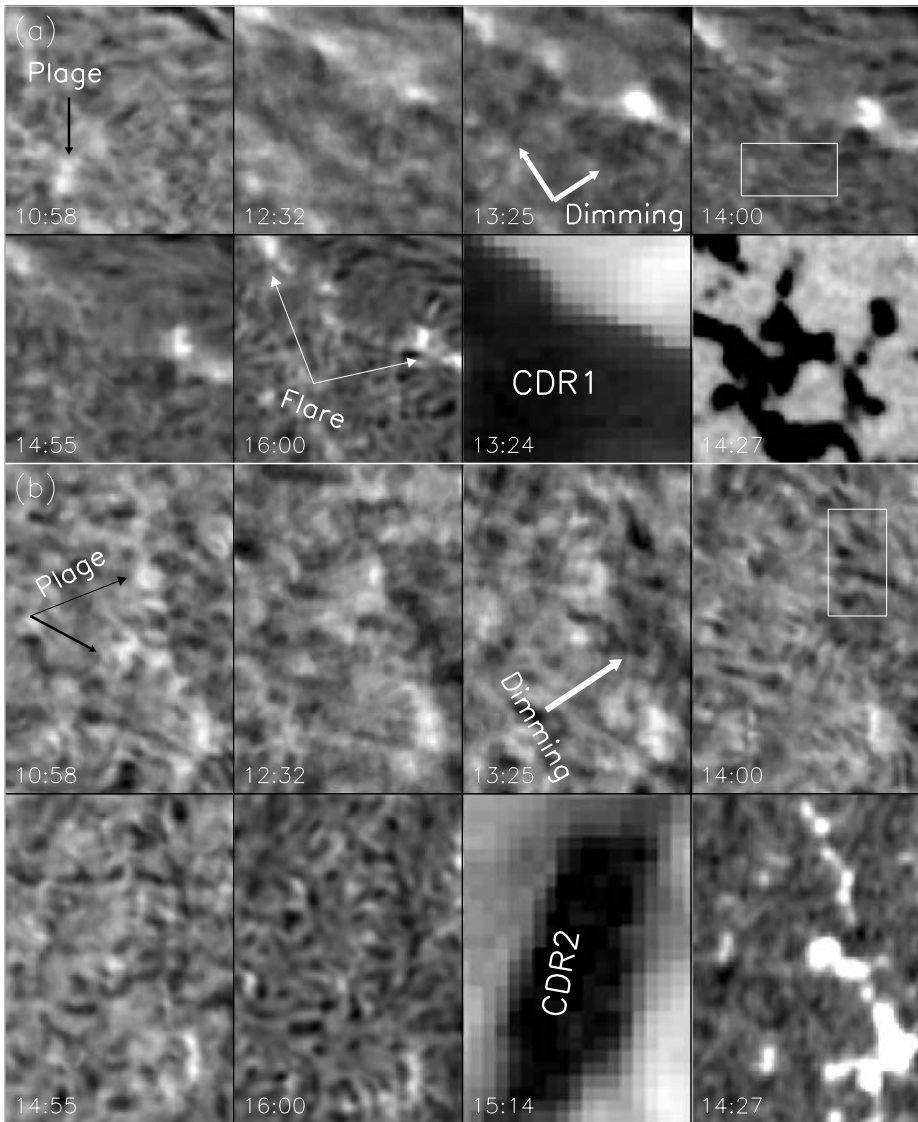
Figure 4 A series of enlarged Hα images below the two coronal dimming regions, CDR1 (a) and CDR2 (b). In (a) and (b), the last frame is an MDI line-of-sight magnetogram and the second frame from the last frame is a soft X-ray image, respectively. The two boxes mark the areas in which the Hα light curves are measured and displayed in Figure 5b. The FOV for (a) and (b) are, respectively, $100'' \times 100''$ and $90'' \times 130''$, which are indicated by the black boxes in Figure 2a.

dimming seen in the soft X-ray image at 10:58 UT. The changes of the Hα flare light curves were similar to the GOES 1–8 Å soft X-ray flux profile, while the intensities of the Hα dimming continuously decreased by about 6 percent.

The sigmoid eruption was possibly associated with a CME, which was first observed by the LASCO C3 coronagraph at 16:08 UT as a full halo event with the leading edge
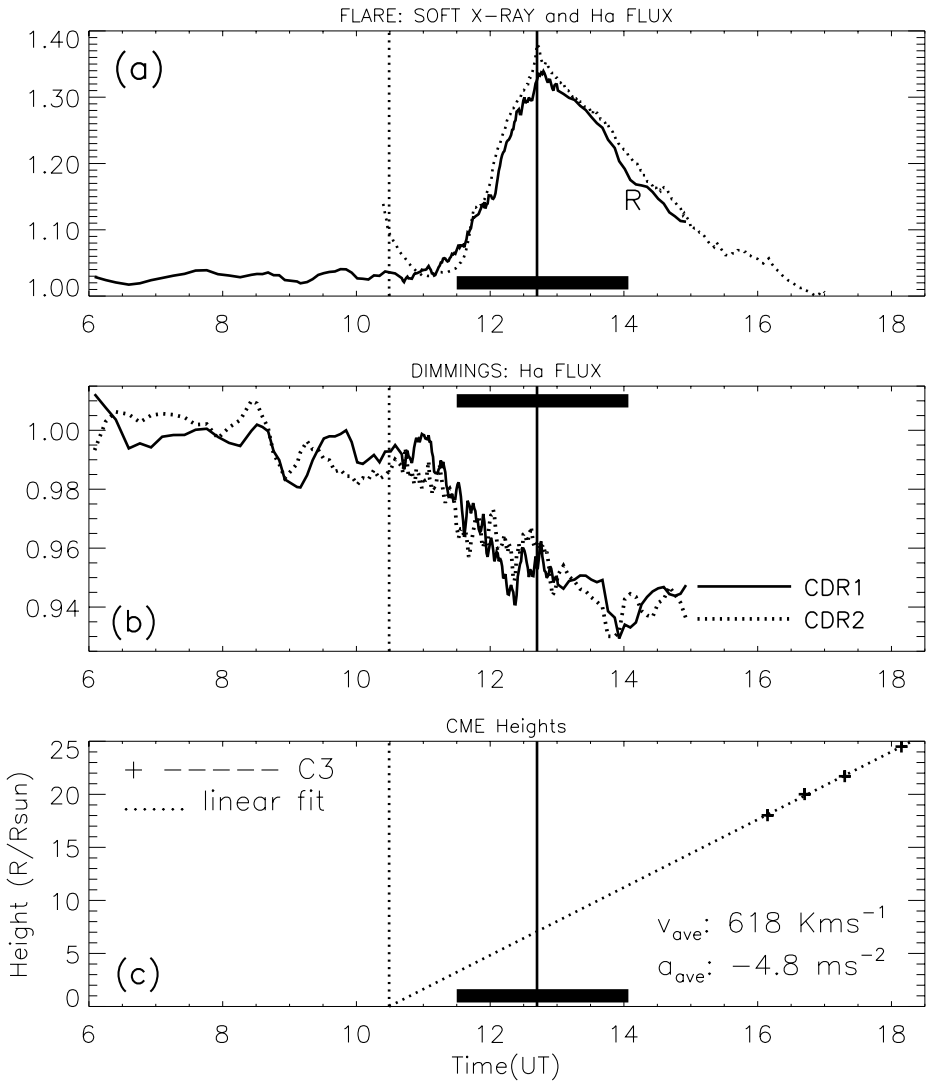
Figure 5 (a) Time profiles of GOES-8 soft X rays in the energy channel of $1-8$ Å (dashed line), and Hα line-center intensity integrated over the box (marked as "R" in Figure 3f) located in one of the Hα flare ribbons (solid lines). (b) Light curves of Hα line-center intensity integrated over the boxes centered on the two dimming regions (marked as "CDR1" and "CDR2" in Figure 3f and indicated by the white boxes in Figure 4). (c) Height of the CME front as a function of time. The value of 1.0 in the Hα light curves indicates the mean Hα intensity of a control area (marked as "CA" in Figure 3f) outside the dimming and brightening regions before the flare start, which are computed from KSO Hα data. The dashed vertical lines indicate the extrapolated onset time of the CME by use of a linear fit, and the solid vertical line shows the peak time of the GOES flare. The horizontal bars indicate the duration of the GOES flare.

some halfway through the C3 field of view. According to S. Yashiro's measurements, the center position angle of the full halo CME was 348°. Unfortunately, only four height – time ($H-T$) points of the CME front can be obtained from the C3 observations owing to missing C2 data. The application of first-order polynomial fitting to the $H-T$ points measured by

S. Yashiro at position angle 38° gives an average speed of 618 km s⁻¹, and the average acceleration from the second-order polynomial fit is -4.8 m s⁻². These parameters are helpful in giving an overall characterization of the CME and are indicated in the lower right corner of Figure 5c. Lack of necessary information of the CME dynamics at its early stage makes it difficult to estimate its onset time. As a very crude approximation, if the average speed is taken to be a constant, then back extrapolation of the CME front from the $H - T$ plots to the solar disk center yields an estimate of the onset time of the CME near 10:30 UT. This is very close to the Hα flare and dimming onset time mentioned above (11:00 UT). Zhang *et al.* (2001) have shown that initiation of a flare-associated CME can occur before the GOES flare onset, with the major acceleration occurring during the rise phase of the GOES flare. Since the coronal sigmoid disturbance, the Hα flare, and dimming started before the GOES flare onset (11:30 UT), it is very likely that the sigmoid activation and subsequent eruption were just the surface activities associated with the CME initiation, and the two dimmings were its on-disk proxy.

4. Conclusions and Discussions

By means of Hα, soft X-ray, EUV, and photospheric magnetic field observations, we studied the sigmoid eruption and coronal bipolar double dimming in association with the C2.3 flare in the quiet sun. Our main results from the observations are summarized as follows. (1) The eruptive sigmoid overlaid the Hα filament channel. The whole filament channel showed no observable changes during the eruption, while the disappearance of the filament section in the channel happened after the eruption. (2) In the course of the eruption, coronal bipolar double dimming was formed around the two ends of the erupted sigmoid, which were located in the regions of opposite magnetic polarities and showed similar shapes in soft X rays and in EIT 195 and 284 Å data. It is evident that the darkening in the coronal dimming regions started when the sigmoid was activated. (3) The chromospheric counterpart of the coronal dimming, the Hα dimming, was detected, and the dimming in EIT 304 Å was also clearly seen. The Hα dimming was formed by the darkening of the Hα bright plages and nearby quiet-sun regions. The occurrence of the sigmoid activation, the earliest Hα dimming, and flare brightening were nearly at the same time, but slightly prior to the GOES flare start. (4) The halo CME observed by the SOHO/LASCO C3 coronagraph was possibly associated with the sigmoid eruption and the bipolar double dimming.

Bipolar double dimming events often appear during eruptive flares in active regions that contain X-ray sigmoid structures or filaments (Hudson and Cliver, 2001). In quiet-sun regions, however, eruptions of sigmoid structures associated with coronal arcade events can also accompany coronal bipolar double dimming. An example of such eruption was shown by Hudson (1999) and Hudson and Cliver (2001) for the event occurring on 23 October 1997. Here we have given another example of a quiet-sun sigmoid eruption in association with coronal bipolar double dimming. We showed that, in addition to the Hα flare, a chromospheric response to the coronal eruption surprisingly occurred in the dimming regions while the underlying Hα filament channel showed no significant changes during the coronal eruption. This is very similar to the cases of sigmoid eruptions in six active regions studied by Pevtsov (2002), in which coronal sigmoids underwent activations and eruptions while underlying Hα filaments were left largely untouched. These examples show that major coronal perturbation may sometimes correspond to only very minor changes in the chromosphere. In the case we studied here, by taking the sigmoid as a coronal sign for a flux rope system, we speculate that the flux rope was possibly located at much greater heights in the corona

but shared the same overlying coronal loops with the underlying Hα filament channel. The sigmoid erupted, opened the overlying coronal loops, escaped from the Sun, and led to the CME. Then the closing-back reconnection of some lower lying open field lines produced the spreading flare ribbons and the postflare arcade. As suggested by Pevtsov (2002), it is very likely that the postflare arcade was formed below the erupted sigmoid and above the filament channel, so that the underlying filament channel can be protected from a disruption. However, the two ends of the flux rope probably rooted deeply in the lower solar atmosphere. In the framework of the flux rope model of CMEs, the coronal bipolar double dimming was explained as the evacuated feet of the magnetic flux rope (Sterling and Hudson, 1997; Zarro *et al.*, 1999; Jiang *et al.*, 2003; Jiang, Li, and Yang, 2006). The appearances of the Hα dimming in this case possibly indicated that the evacuated feet of the flux rope can deeply extend into the chromosphere.

Since the dimming was simultaneously observed in Hα, EUV, and soft X rays, it was more likely due to a loss in density rather than a change in the temperature of the coronal plasma. Otherwise, brightening instead of dimming would be observed as the soft X-ray material cools through 10^4 K. If the two dimming regions represent loss of the coronal mass sweeping into the CME observed by the LASCO, the lost material may have originated from the deeper and denser chromosphere and may have a relatively large temperature range, from about 10^4 K to several 10^6 K. However, we would like to point out that the formation of the complicated Hα line is involved in large height and wide temperature ranges. Details of the effect of the pressure drop from the flux rope expansion on the Hα line formation is needed from further theoretical work. Like the event of 19 October 2001 (Jiang *et al.*, 2003), it is noted that the location and morphological evolution of the Hα dimming were also different from the flare nimbus phenomenon (Ellison, Mckenna, and Reid, 1961) and the Hα darkening discussed by Neidig *et al.* (1997), which lay over "magnetically neutral" areas bordered by ridges of opposite polarity fields during major flares. We also note that the Hα dimming took the form of bipolar double dimming in both the 19 October 2001 event and the event we studied here. Since only two examples were studied at present, many questions are still open about Hα dimming phenomena. For example, do they have other geometries? Can we detect their corresponding changes in the photosphere, such as photospheric dimming or associated changes of photospheric magnetic fields? Further observations are required to clarify these questions.

References

Brueckner, D.E., *et al.*: 1995, *Solar Phys.* **162**, 357.
Delaboudiniére, J.-P., *et al.*: 1995, *Solar Phys.* **162**, 291.
Ellison, M.A., Mckenna, S.M.P., Reid, J.H.: 1961, *Mon. Not. Roy. Astron. Soc.* **122**, 491.
Gopalswamy, N., Hanaoka, Y.: 1998, *Astrophys. J.* **498**, L179.
Harra, L.K., Sterling, A.C.: 2001, *Astrophys. J.* **561**, L215.
Harrison, R.A., Lyons, M.: 2000, *Astron. Astrophys.* **358**, 1097.
Hudson, H.S.: 1999, *Solar Phys.* **190**, 91.
Hudson, H.S., Acton, L.W., Freeland, S.L.: 1996, *Astrophys. J.* **470**, 629.
Hudson, H.S., Cliver, E.W.: 2001, *J. Geophys. Res.* **106**, 199.
Hudson, H.S., Webb, D.F.: 1997, In: Crooker, N., Joselyn, J., Feynman, J. (eds.) *Coronal Mass Ejections*, *Geophysical Monograph*, vol. **99**, American Geophysical Union, Washington, p. 27.

Jiang, Y.C., Ji, H.S, Wang, H.M, Chen, H.D.: 2003, *Astrophys. J.* **597**, L161.

Jiang, Y.C., Li, L.P., Yang, L.H.: 2006, *Chin. J. Astron. Astrophys.* **6**, 345.

Jiang, Y.C., *et al.*: 2006, *New Astron.* **11**, 612.

Martin, S.F.: 1998, *Solar Phys.* **182**, 107.

Martin, S.F., Bilimoria, R., Tracadas, P.W.: 1994, In: Rutten, R., Schrijver, C.J. (eds.) *Solar Surface Magnetism*, Kluwer Academic Publishers, Dordrecht, p. 303.

Neidig, D.F., Švestka, Z., Cliver, E.W., Airapetian, V., Henry, T.W.: 1997, *Solar Phys.* **170**, 321.

Pevtsov, A.A.: 2002, *Solar Phys.* **207**, 111.

Pevtsov, A.A., Canfield, R.C., Zirin, H.: 1996, *Astrophys. J.* **473**, 533.

Scherrer, P.H., *et al.*: 1995, *Solar Phys.* **162**, 129.

Steinegger, M., *et al.*: 2000, In: Wilson, A. (ed.) *The Solar Cycle and Terrestrial Climate, ESA SP-463*, European Space Agency, Noordwijk, The Netherlands, p. 617.

Sterling, A.C., Hudson, H.S.: 1997, *Astrophys. J.* **491**, L55.

Thompson, B.J., Plunkett, S.P., Gurman, J.B., Newmark, J.S., St. Cyr, O.C., Michels, D.J.: 1998, *Geophys. Res. Lett.* **25**, 2465.

Thompson, B.J., *et al.*: 2000, *Geophys. Res. Lett.* **27**, 1431.

Tsuneta, S., *et al.*: 1991, *Solar Phys.* **136**, 37.

Wang, H., *et al.*: 2000, *Astrophys. J.* **536**, 971.

Zarro, D.M., Sterling, A.C., Thompson, B.J., Hudson, H.S., Nitta, N.: 1999, *Astrophys. J.* **520**, L139.

Zhang, J., Dere, K.P., Howard, R.A., Kundu, M.R., White, S.M.: 2001, *Astrophys. J.* **559**, 452.

Zirker, J.B., Martin, S.F., Harvey, K., Gaizauskas, V.: 1997, *Solar Phys.* **175**, 27.